A Large Multimodal Molecular Representation Encoder-Decoder Foundation Model for Chemistry

Victor Y. Shirasuna
IBM Research Brazil
Rio de Janeiro, RJ, Brazil
vshirasuna@ibm.com

Emilio Vital Brazil
IBM Research Brazil
Rio de Janeiro, RJ, Brazil
evital@br.ibm.com

Eduardo Soares
IBM Research Brazil
Rio de Janeiro, RJ, Brazil
eduardo.soares@ibm.com

Nathaniel Park
IBM Research Almaden
San Jose, CA, USA
npark@us.ibm.com

Dmitry Zubarev
IBM Research Almaden
San Jose, CA, USA
dmitry.zubarev@ibm.com

Vidushi Sharma
IBM Research Almaden
San Jose, CA, USA
vidushis@ibm.com

Indra Priyadarsini
IBM Research Tokyo
Tokyo, Japan
indra.ipd@ibm.com

Caio Gama
IBM Research Brazil
Rio de Janeiro, RJ, Brazil
caiogama@ibm.com

Enzo Oliveira
IBM Research Brazil
Rio de Janeiro, RJ, Brazil
Enzo.Reis@ibm.com

Abstract

Most large-scale chemical language models are trained on a single textual molecular representation using self-supervised learning over large unlabeled corpora. These models excel in tasks such as property prediction and molecule generation by learning contextualized representations of input tokens. However, relying solely on one representation may result in the loss of structural or semantic information captured by alternative formats and may limit the model's ability to generalize across diverse molecular encodings. To address this limitation, we incorporate multiple textual molecular representations—including SMILES, SELFIES, molecular formula, IUPAC name, International Chemical Identifier (InChI), serialized polymer graph (SPG), and electrolyte formulations in an unified vocabulary to harness the unique strengths of each format. Here, we introduce a large encoder-decoder chemical foundation model based on the Bamba architecture, a hybrid of Transformers and Mamba-2 layers, designed to support multi-representational inputs. The model is pre-trained in a BERT-style on 588 million samples, resulting in a corpus of approximately 29 billion molecular tokens. These models serve as a foundation for language chemical research in supporting different complex tasks, including molecular properties prediction, classification, and molecular translation. Furthermore, extensive studies of the multimodal molecular latent space indicate cross-representation alignment and reveal how different textual encodings of the same molecule can converge toward a unified semantic representation. This shared space may facilitate deeper insights into molecular structure, enhance generalization, and support a broad range of downstream applications.

1 Introduction

The development of large-scale pre-training methodologies for chemical language models (LMs) constitutes a significant advancement in the field of cheminformatics (1). These methodologies demonstrate a notable efficacy in addressing complex molecular tasks, including the prediction of

properties and the generation of molecules (2; 3). The effectiveness of these models is mainly due to their ability to acquire contextualized representations of input tokens through self-supervised learning on extensive unlabeled corpora (4).

With the advance of the Transformers architecture, several chemical models have been proposed to leverage attention as its core module (5; 6; 7; 8; 9). The effectiveness of self-attention is attributed to its ability to route information densely within a context window (10), allowing it to model complex data (11). However, this property presents essential limitations, such as the inability to model anything outside of a finite window and the quadratic scaling with respect to the window length (12). A considerable amount of research has emerged on more efficient variants of attention to overcome these drawbacks (13).

In particular, structured state-space sequence models (SSMs) have been introduced as a promising class of architectures to support much longer context lengths for sequence modeling (14). These models can be interpreted as a combination of recurrent neural networks (RNNs) and convolutional neural networks (CNNs) (15). The Mamba model is a simplified end-to-end SSM-based neural network architecture without attention or even MLP blocks (16). In this context, recent approaches have demonstrated the efficiency and capability of SSMs in learning a chemical language better than or comparable to Transformer-based models (17). To address the limitations and harness the advantages of the self-attention and state-space modules, recent works have proposed a hybrid architecture of Transformer and Mamba-2 layers for general large language models (LLMs) (18; 19; 20).

Most of the proposed chemical foundation models rely solely on a single representation or require the adaptability of a new notation for model compatibility. Common molecular representations the models are trained on include SMILES, SELFIES, and PSMILES. However, the use of specific notation may limit the ability of the model to generalize across diverse molecular encodings. Furthermore, diverse molecular notations may complement important molecular information that a specific one does not contain. For PSMILES we used the serialized polymer graph (SPG) representation since it could accommodate both a broad array of polymer architectures and be easily interoperable with existing literature datasets—simplifying assembly of pre-training and benchmarking datasets (21).

In this study, we present a novel hybrid architecture of a large general string-based molecular foundation model of the Transformer and Mamba-2 layers, denoted STR-Bamba$_{426M}$. Our STR-Bamba$_{426M}$ encoder-decoder foundation model leverages multiple molecular string textual representations in a single vocabulary using an efficient attention and SSM-based model. Our main contributions are:

- We pre-train a large-scale encoder-decoder foundation model for molecules, denoted STR-Bamba$_{426M}$, on more than 117 million small molecules from PubChem (22), 2 million synthetic and real polymers from the literature (21), and 258 electrolyte formulations (23), resulting in 119 million unique molecules. With the multimodal setting, the total training data is composed of 588 million samples, which is equivalent to 29 billion molecular tokens.

- A special custom tokenizer for enconding the different molecular representations individually. We built a custom tokenizer to handle each modality properly in a single unified vocabulary of molecular textual representations.

- Our STR-Bamba$_{426M}$ foundation model is an inference-efficiency hybrid Transformer and Mamba-2 base model of 426 million parameters. The design of the model architecture allows for the use of longer context lengths, opening space to leverage multiple molecular representations into a single input. All used code and checkpoints for these models are in progress to be fully open-sourced.

- We perform extensive experimentation on several classification and regression property prediction tasks from 27 benchmark datasets, covering a wide range of tasks for small molecules, and polymer molecules. We also study the quality of the latent space created by the STR-Bamba$_{426M}$ model to represent the multimodal setting of molecular representations. Furthermore, an evaluation of the capabilities of the encoder-decoder configuration of the proposed architecture is conducted by translating different molecular formats of the same molecule.

2 Overview of the proposed approach

The following detail the proposed approach of the STR-Bamba architecture to leverage the multimodal molecular textual representations setting in a unified vocabulary and model.
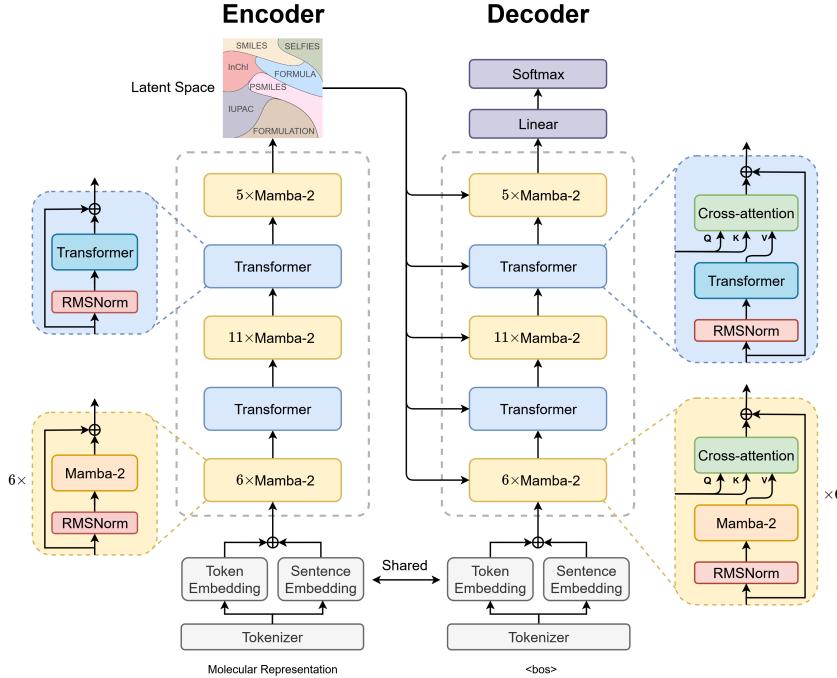

Figure 1: This figure illustrates the general architecture of the base STR-Bamba$_{426M}$ model.

Tokenization: A custom tokenizer was carefully built to encode the seven different molecular representations supported by STR-Bamba appropriately. Specifically, we employed the Byte-Pair Encoding (BPE) tokenization for the main encoding process, and a pre-tokenizer step is performed to handle each modality individually. To identify each modality, we considered the special token representations, i.e., *<smiles>* for SMILES, *<selfies>* for SELFIES, *<iupac>* for IUPAC name, *<inchi>* for InChI, *<formula>* for molecular formula, *<polymer_spg>* for SPG, and *<formulation_start>* for electrolyte formulations.

For SMILES, SELFIES and SPG we used the regular expression from (24) to split in an atom-wise approach since it has been extensively used for molecular models (25; 26; 27; 9). For the molecular formula and InChI notations, we first extract the numbers associated with the atoms. Finally, formulations use the same atom-wise tokenization with the addition of recognizing formulation compositions. Although the IUPAC name is not preprocessed beforehand, the BPE appropriately encodes the high-frequency pieces of the name. We trained the tokenizer with 5% of the total training data, resulting in approximately 28 million samples for all molecular modalities. The size of the constructed vocabulary yields 5000 tokens, with 13 special tokens and 4987 molecular tokens.

Pre-training Data: A combination of small and polymer molecules, and electrolyte formulation data was used to compose our training data. The data on small molecules were extracted from the PubChem database, resulting in a total of 118 million molecules. However, since it does not contain the SELFIES representations, we generated the SELFIES format from the SMILES notation. Hence, the remaining data consist of 117 million molecules with a minimum loss of the total extracted data.

The collection of polymer data for pre-training is a composition of synthetics with experimental datasets, forming a dataset of approximately 2 million polymer structures. The use of generated polymer data is known to contain non-viable polymer structures. Hence, the pre-training data were carefully pooled from a selection of open literature sources, (28; 29; 30; 31; 32; 33; 34; 35; 36; 37; 38; 39), avoiding whenever possible, datasets containing potentially problematic structure. We also

enriched the training data with an additional 258 electrolyte formulations. Therefore, the total dataset size for pre-training the STR-Bamba$_{426M}$ model comprises approximately 588 million samples. From this total, each of the five molecular modalities from PubChem is used, resulting in 585M samples added with the polymer and formulation data.

Model Architecture: STR-Bamba$_{426M}$ is an encoder-decoder model built on the Bamba architecture [1], an inference-efficient hybrid approach of Transformer and Mamba-2. This architecture leverages the strengths of both attention and state-space mechanisms. We slightly modified the Bamba architecture to handle multiple molecular representations and exploit the multimodal setting into a single unified vocabulary and model, which are shown in Fig. 1. The model configuration for the base architecture, Mamba-2, and Transformer used in our implementation is shown in Table 1.

Table 1: STR-Bamba$_{426M}$ base architecture specificity.

Hidden size	Layers	lr start	Vocab size	Dataset size	# tokens	# Encoder	# Decoder	Total params
1024	24	3e-5	5000	119M	29B	163M	263M	426M

	d state	d conv	head dim	expand factor	dt min	dt max	dt init floor	
	128	4	64	2	0.001	0.1	1e-4	

attn layer index	head dim	num heads	num heads kv	out proj bias	qkv proj bias	rotary emb size
6, 18	64	16	8	false	false	64

To align different representations of the same molecule, we performed a modification of the embedding layer similar to the BERT model. To achieve this, we trained the encoder with an aggregation of token and sentence embeddings. The token embedding learns to encode each molecular token properly, and the sentence embedding learns to align one molecular input concatenated to another or a series of representations separated by the *<sep>* special token. In addition, there is no need to add positional encodings after the embedding layer, since Mamba operates in a recurrent way. Finally, the embeddings are shared between the encoder and the decoder to take advantage of the embeddings learned from the encoder.

Following the Bamba model specificity, we placed two attention layers at the beginning and end of the total of 24 layers. Specifically, one attention is followed by 6 layers of Mamba-2 and the other by 18 layers. Additionally, Grouped Query Attention (GQA) and Rotary Position Embeddings (RoPE) are employed in the attention mechanisms to improve training and inference efficiency without losing performance. The use of RoPE embeddings is also exploited to further optimize the relative encoding through position-dependent rotations R_m of the query and keys at position m. These rotations can be implemented as pointwise multiplications and do not significantly increase computational complexity as shown in Eq. (1).

$$Attention_m(Q, K, V) = \frac{\sum_{n=1}^{N} \langle \varphi(R_m q_m), \varphi(R_n k_n) \rangle \, v_n}{\sum_{n=1}^{N} \langle \varphi(q_m), \varphi(k_n) \rangle} \tag{1}$$

where Q,K,V are the query, key and value, respectively, and φ is a random feature map.

Since the base Bamba architecture is a decoder-only model, we also added a cross-attention layer after each Mamba-2 and Transformer layers of the decoder to construct an effective encoder-decoder architecture. The addition of the cross-attention layer is incorporated to generate valid molecular notations conditioned with the embeddings from the encoder. In the implementation, we used the same cross-attention mechanism as in the BART model, receiving the contextual queries and keys from the encoder's embeddings (40).

For the state-space layers, we specifically used the Mamba-2 architecture (41). The Mamba-2 is an improvement of the original Mamba work by simultaneously allowing much larger state dimensions and reducing the training. The Mamba models originate from a continuous-time system that maps an input function or sequence $x(t) \in \mathbb{R}^M$ to an output response signal $y(t) \in \mathbb{R}^O$ through an implicit latent state $h(t) \in \mathbb{R}^N$ which can be mathematically formulated using the following ordinary differential equations.

---

[1]https://huggingface.co/blog/bamba

$$h'(t) = Ah(t) + Bx(t),$$
$$y(t) = Ch(t) + Dx(t) \tag{2}$$

where $A \in \mathbb{R}^{N \times N}$ and $C \in \mathbb{R}^{O \times N}$ control how the current state evolves over time and translates to the output, $B \in \mathbb{R}^{N \times M}$ and $D \in \mathbb{R}^{O \times M}$ depict how the input influences the state and the output, respectively.

The tokens extracted from the molecular representations through the hybrid Transformer and SSM encoder are embedded in a 1024-dimensional space. Furthermore, each encoder-decoder layer is designed to process the molecular token embeddings, represented as $\mathbf{x} \in \mathbb{R}^{T \times L}$, where T denotes the input tokens, and L represents the dimension of the embedding space. The length of T has no theoretical limit except for hardware limitations, which opens space to leverage multiple representations in a single input string text.

Pre-training strategies: The STR-Bamba$_{426M}$ model was pre-trained in a two-stage strategy. We first train the encoder part to construct a strong embedding space representation for all molecular modalities. Finally, the decoder is trained using the contextual representation of the encoder to correctly predict the next token generation. We used 396 and 8 NVIDIA A100 (40GB) GPUs to train phase 1 and phase 2, respectively. Each phase is described in the following:

- Phase 1 consists of training only the encoder to better learn to encode and align different molecular formats. We employ a similar strategy defined in (42) using token and sentence embedding. The token embedding processes the molecular tokens, while the sentence embedding handles a boolean value for each token to assess whether a molecular format *B* is equivalent to format *A* for depicting the same molecule. We also used the masked language model from (42) to train in a self-supervised way. Thus, the objective of encoder training is to learn to correctly classify masked tokens and to determine if the different molecular formats *A* and *B* are the same molecule or not.

- Phase 2 consists of training only the decoder by generating a valid molecular representation given the contextual embeddings of the encoder. To achieve this, we build a batch consisting of reconstructing the input molecule format with the addition of two representations randomly selected of the same molecule. Representations that do not have more than one format are trained to only reconstruct the input text.

3 Experiments

To evaluate the capability of the STR-Bamba$_{426M}$ model in harnessing all molecular modalities, we performed a series of experiments for all types of molecular notation. An analysis of the latent space is performed to evaluate the effectiveness of the encoder in representing each molecular modality appropriately. For this, we plotted the latent space with t-SNE using 2000 random samples of each modality, except for the electrolyte formulation, we used all 258 samples. A K-means algorithm was used to cluster the semantic regions by varying the number of clusters from 2 to 10. The goal is to evaluate whether a clustering algorithm is capable of recognizing the seven different representations the model supports. For this experiment, we evaluated it using the following clustering metrics: Davies-Bouldin Index, Adjusted Rand Index, V-Measure, and Fowlkes-Mallows Score.

We also evaluated the performance of the STR-Bamba$_{426M}$ model on a wide range of property prediction tasks on 27 datasets, giving a total of 97 tasks. To assess the performance of the model on the data trained in the PubChem database in downstream tasks, we used the MoleculeNet benchmark. To take advantage of the multimodal setting of molecular representations, we assessed each individual and a combination of modalities in the same input text combining the molecular information strengths of each. Thus, we determined all possible combinations between formats and performed an optimization with the Tree-Structured Parzen Estimator (TPE) algorithm using the validation set to find the top-3 combinations for each task.

To evaluate the performance of property predictions for polymer structures, we employed a variety of benchmark datasets sourced from the existing literature. All experiments were carried out with five different seeds to ensure the statistical relevance of the results. In addition, to ensure an

unbiased assessment, we maintained consistency with the original benchmark by adopting identical train/validation/test splits for all tasks. Detailed specification for each benchmark dataset and evaluation metrics used is provided in the Supplementary Materials.

Finally, the encoder-decoder architecture of STR-Bamba enables a wide range of tasks. Therefore, we also assessed the ability of the decoder to translate a molecular representation into another in the same molecule. For this, we evaluated the model on 3007 random molecules from the training data to generate valid and structure similarity SMILES and SELFIES using the *RDKit*[2] library and tanimoto similarity, respectively. Additionally, the generation of the IUPAC name text and the molecular formula was assessed using the BLEU-1, BLEU-2 and Jaccard similarity.

4 Results and Discussion

In this section, we provide a wide range of experimental results for the STR-Bamba$_{426M}$ architecture, accompanied by a discussion. The experiments consist of: i) A latent space analysis of multiple molecular representation; ii) Performance assessment on various property prediction tasks; iii) Translation of different representations of the same molecule.

4.1 Latent space study

To evaluate the effectiveness of the encoder in learning the seven molecular representations, the K-means clustering algorithm is used to delimit the different regions in the latent space. Figure 2a shows the projection of the t-SNE of the encoder embeddings for each molecular format and Fig. 2b shows seven clusters determined by the K-means algorithm.
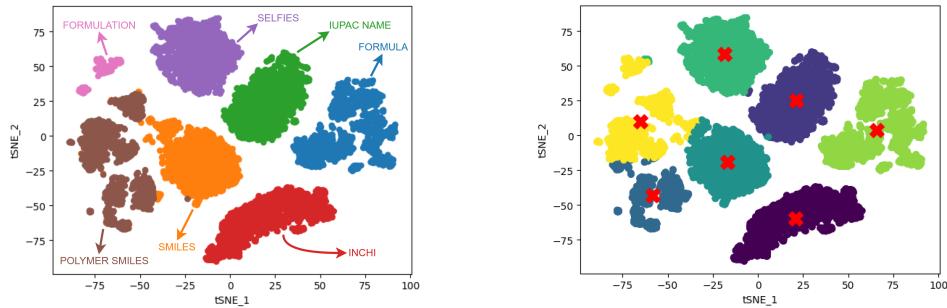
(a) Latent space of the 7 different molecular modalities. (b) Identified clusters using the K-means algorithm.

Figure 2: Latent space analysis of multiple molecular representation.

Table 2: Performance of K-means latent space clustering.

Number of clusters (n)	n=2	n=3	n=4	n=5	n=6	n=7	n=8	n=9	n=10
Davies-Bouldin Index ↓	1.18	0.87	0.73	0.75	0.81	0.70	**0.69**	0.71	0.71
Adjusted Rand Index ↑	0.26	0.41	0.61	0.74	0.84	**0.91**	0.84	0.79	0.79
V-Measure ↑	0.43	0.57	0.74	0.82	0.88	**0.92**	0.88	0.87	0.87
Fowlkes-Mallows Score ↑	0.51	0.58	0.71	0.80	0.86	**0.92**	0.87	0.83	0.83

In Table 2 the number of clusters is varied between distinct clustering metrics to systematic determine the best number of regions. The Davies-Boulding Index shows that eight clusters yield the most perfect match followed by seven, nine, and ten regions, respectively. Similarly, the Adjusted Rand Index, V-Measure, and Fowlkes-Mallows Score exhibit the best delimitation by seven clusters. This shows that by clustering the latent space achieves the same number of molecular representations as STR-Bamba$_{426M}$ supports.

It is noteworthy that the metrics employed suggest that eight clusters also have a good clustering determination. This can be seen as the PSMILES represented by the SPG notation and SMILES have an intersection, which is seen to be natural since both have similar textual appearances with slightly different notation.

---

[2]https://www.rdkit.org

6

4.2 Comparison with SOTA on property prediction benchmarking tasks

MoleculeNet benchmark: An assessment of the learned multimodal latent space for property prediction is conducted for small molecules using the MoleculeNet benchmark across various tasks. For our model, we individually tested each molecular representation and the top-3 combination of formats. Detailed results for all individual and combined notations tested, and a full comparison with SOTA models can be found in the Supplementary Materials.

For classification tasks, the STR-Bamba$_{426M}$ model outperformed five of the six downstream tasks compared to the SOTA models. The ClinTox dataset was the only task surpassed by another model, which is the MetaGIN architecture, a graph-based model. Although the MetaGIN model achieved the best performance in the ClinTox task, our model reached the second-best performance. Furthermore, the variation in MetaGIN results is considerable high with a ROC-AUC average of 90.8%. In contrast, the STR-Bamba model achieved an ROC-AUC average of 96.44% with a very slight variation between different seeds. This can demonstrate some instability of the MetaGIN model in this task, which can occasionally outperform STR-Bamba on the ClinTox task.

Although the STR-Bamba$_{426M}$ model outperformed two of five regression tasks, the model obtained very close results compared to the SOTA models. Our model achieved outstanding performance in the ESOL and FreeSolv tasks. Additionally, it achieved the second best performing model for the ESOL task with the pre-trained model and QM9 dataset with the fine-tuned model.

These results demonstrate the ability of the hybrid approach to perform better or have performance comparable to Transformer-based or SSM-based only models by leveraging multiple formats. Finally, in nine out of 11 downstream tasks evaluated on the MoleculeNet benchmark, the combination of molecular representations obtained the best results with the STR-Bamba$_{426M}$ model. This demonstrates the importance of taking advantage of the strengths of each modality in a unified model.

Polymer benchmarks: The STR-Bamba$_{426M}$ model was also evaluated in a wide range of polymer property prediction tasks from the literature. Thus, Figure 3 shows the results in 17 downstream tasks in which the normalized error is considered to assess the model compared to the SOTA models. Similarly, we conducted more 9 polymer property prediction tasks in which the R^2 metric was used, resulting in a total of 26 downstream tasks for polymer structures. The results obtained from Fig. 3 and the results of the 9 mentioned polymer prediction tasks are detailed in the Supplementary Materials.
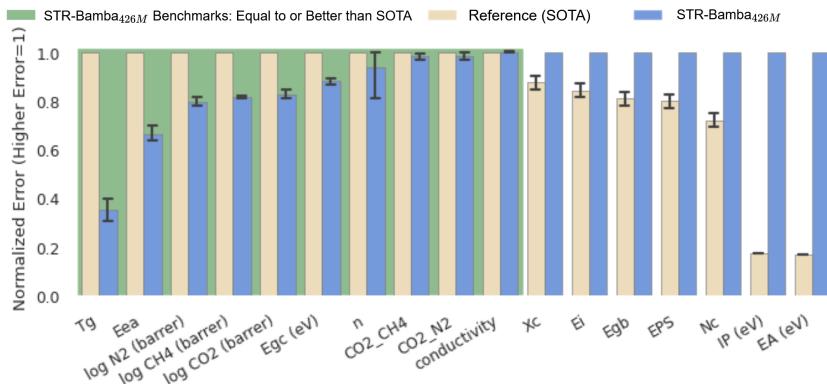
Figure 3: Comparison of the STR-Bamba$_{426M}$ model with state-of-the-art models across various polymer property predictions. The results show that STR-Bamba$_{426M}$ outperforms SOTA models in **10 out of 17 properties**. The errors are normalized such that a value of 1 represents the maximum error observed in the comparison.

In all 26 polymer tasks, the STR-Bamba$_{426M}$ model outperformed or reached near-state-of-the-art results in 17 downstream tasks. In Fig. 3 with the tasks in which the error was used to evaluate the models, the green area on the left shows that the model was equal or better than the SOTA models in 10 of 17 property prediction tasks. In the nine remaining polymer tasks, especially for polymer membrane tasks, the STR-Bamba$_{426M}$ model notably outperformed the models documented in the

literature. In tasks $T_{d\frac{1}{2}}$ and $\log(P_{CO_2})$, the pre-trained model achieved a better performance than SOTA models with an additional improvement from fine-tuned models.

Finally, for the gas permeability of polymer tasks (CalTech), the STR-Bamba$_{426M}$ model was capable of outperforming or achieving SOTA results in 4 out of 6 tasks and achieved the second best performance for the remaining two tasks. Although STR-Bamba did not surpass the DNN ensemble(MFFs) model on the O_2 task with a R^2 of 0.92, it reached a very close performance with a R^2 average of 0.91. Similarly, for the CO_2 task, our model achieved an average R^2 of 0.90, while the SPG-TED$_{289M}$ obtained a R^2 of 0.91. This may illustrate the richness capability of the latent space of STR-Bamba in learning multiple molecular formats. Therefore, the shared common space of diverse chemical representations may enhance the molecular prediction, in which the SMILES share some properties with SPG as seen in the latent space study.

4.3 Representation translation

The encoder-decoder architecture setting of STR-Bamba gives flexibility to a range of downstream tasks. Hence, we also evaluated the performance of the STR-Bamba$_{426M}$ model in translating between different representations of the same molecule. The results of translating a representation to SMILES and SELFIES are shown in Fig. 4a, while the translation of a representation to IUPAC name and molecular formula are shown in Fig. 4b.

(a) Translation to SMILES and SELFIES. (b) Translation to IUPAC and molecular formula.
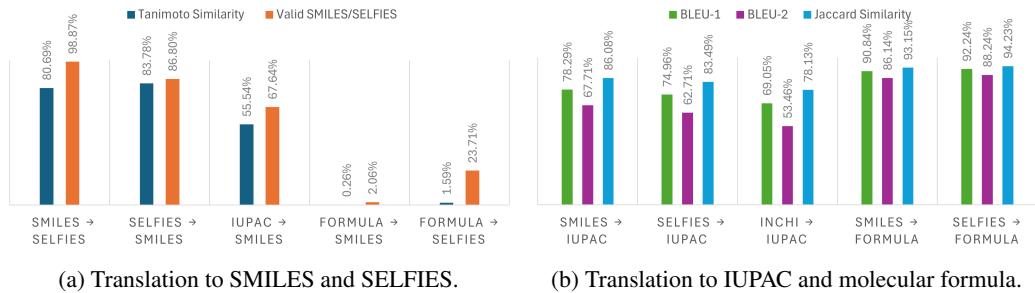
Figure 4: Translation of different molecular representations.

As the decoder training was conducted without using the entire training data, all results show with a few-shot learning approach. For translating from SMILES to SELFIES and vice versa, the representations achieved the best structural and validity generation, which can be explained that SELFIES is a notation derived from SMILES notation. Similarly, the IUPAC name format may generate a similar SMILES notation but with less structure and valid molecules guarantees. In addition, the model was tasked with generating SMILES and SELFIES from the molecular formula notation. This can be a challenging task due to multiple valid molecules with different structure properties that can be composed from the molecular formula. However, it is noteworthy that the SELFIES notation generated a considerable number of valid molecules compared to SMILES since this representation was developed to be a robust molecular representation.

The task of generating the molecular formula from SMILES and SELFIES achieved results very close to the original formula. In particular, the translation from the SELFIES notation was slightly better compared to SMILES representation. However, generating the IUPAC name was a more difficult task. The SMILES notation achieved the best results from this task, whereas the InChI achieved the lowest. In general, the performance achieved in the representation translation task shows the potential ability of the STR-Bamba$_{426M}$ model to generate similar and valid molecular representations in the same molecule. The proposed architecture of multiple molecular formats in a unified latent space helps the model align the different modalities in generation tasks.

5 Conclusion

This paper introduces the STR-Bamba$_{426M}$ model, a multimodal textual molecular representation foundation model of a hybrid Transformer and Mamba-2 architecture capable of encoding multiple molecular notations in a single model. A custom tokenizer was developed to allow the encoding of

each modality appropriately for the model. Additionally, the STR-Bamba architecture allows for the aggregation of multiple representations in a single text input, as it does not contain any token length limitation, except for hardware limitations.

Extensive experimentation with prediction of the molecule properties of small molecules, and polymers achieved competitive results by leveraging the multimodal setting compared to state-of-the-art models. Furthermore, the latent space analysis demonstrates the model's capability to represent each molecular format. Finally, the encoder-decoder architecture allows multiple tasks, such as translating between representations of the same molecule, showing the potential to walk between modalities.

Acknowledgments and Disclosure of Funding

References

[1] A. V. Sadybekov and V. Katritch, "Computational approaches streamlining drug discovery," *Nature*, vol. 616, no. 7958, pp. 673–685, 2023.

[2] J. Ross, B. Belgodere, V. Chenthamarakshan, I. Padhi, Y. Mroueh, and P. Das, "Large-scale chemical language representations capture molecular structure and properties," *Nature Machine Intelligence*, vol. 4, no. 12, pp. 1256–1264, 2022.

[3] E. Soares, F. Cipcigan, D. Zubarev, and E. V. Brazil, "A framework for toxic pfas replacement based on gflownet and chemical foundation model," in *NeurIPS 2023 AI for Science Workshop*, 2023.

[4] R. Bommasani, D. A. Hudson, E. Adeli, R. Altman, S. Arora, S. von Arx, M. S. Bernstein, J. Bohg, A. Bosselut, E. Brunskill *et al.*, "On the opportunities and risks of foundation models," *arXiv preprint arXiv:2108.07258*, 2021.

[5] G. Pesciullesi, P. Schwaller, T. Laino, and J.-L. Reymond, "Transfer learning enables the molecular transformer to predict regio-and stereoselective reactions on carbohydrates," *Nature communications*, vol. 11, no. 1, p. 4874, 2020.

[6] S. Chithrananda, G. Grand, and B. Ramsundar, "Chemberta: large-scale self-supervised pretraining for molecular property prediction," *arXiv preprint arXiv:2010.09885*, 2020.

[7] N. Janakarajan, T. Erdmann, S. Swaminathan, T. Laino, and J. Born, "Language models in molecular discovery," *arXiv preprint arXiv:2309.16235*, 2023.

[8] E. Soares, E. V. Brazil, K. F. A. Gutierrez, R. Cerqueira, D. Sanders, K. Schmidt, and D. Zubarev, "Beyond chemical language: A multimodal approach to enhance molecular property prediction," *arXiv preprint arXiv:2306.14919*, 2023.

[9] E. Soares, E. V. Brazil, V. Shirasuna, D. Zubarev, R. Cerqueira, and K. Schmidt, "An open-source family of large encoder-decoder foundation models for chemistry," *Communications Chemistry*, vol. 8, no. 1, 7 2025. [Online]. Available: https://www.nature.com/articles/s42004-025-01585-0#citeas

[10] A. Vaswani, N. Shazeer, N. Parmar, J. Uszkoreit, L. Jones, A. N. Gomez, Ł. Kaiser, and I. Polosukhin, "Attention is all you need," *Advances in neural information processing systems*, vol. 30, 2017.

[11] Y. Tay, M. Dehghani, D. Bahri, and D. Metzler, "Efficient transformers: A survey," *ACM Computing Surveys*, vol. 55, no. 6, pp. 1–28, 2022.

[12] T. Lin, Y. Wang, X. Liu, and X. Qiu, "A survey of transformers," *AI open*, vol. 3, pp. 111–132, 2022.

[13] E. Kotei and R. Thirunavukarasu, "A systematic review of transformer-based pre-trained language models through self-supervised learning," *Information*, vol. 14, no. 3, p. 187, 2023.

[14] A. Gu, K. Goel, and C. Ré, "Efficiently modeling long sequences with structured state spaces," *arXiv preprint arXiv:2111.00396*, 2021.

[15] J. T. Smith, A. Warrington, and S. W. Linderman, "Simplified state space layers for sequence modeling," *arXiv preprint arXiv:2208.04933*, 2022.

[16] A. Gu and T. Dao, "Mamba: Linear-time sequence modeling with selective state spaces," *arXiv preprint arXiv:2312.00752*, 2023.

[17] E. Soares, E. V. Brazil, V. Shirasuna, D. Zubarev, R. Cerqueira, and K. Schmidt, "A Mamba-based foundation model for materials," *npj Artificial Intelligence*, vol. 1, no. 1, 6 2025. [Online]. Available: https://www.nature.com/articles/s44387-025-00009-7

[18] O. Lieber, B. Lenz, H. Bata, G. Cohen, J. Osin, I. Dalmedigos, E. Safahi, S. Meirom, Y. Belinkov, S. Shalev-Shwartz, O. Abend, R. Alon, T. Asida, A. Bergman, R. Glozman, M. Gokhman, A. Manevich, N. Ratner, N. Rozen, E. Shwartz, M. Zusman, and Y. Shoham, "Jamba: A hybrid transformer-mamba language model," 2024. [Online]. Available: https://arxiv.org/abs/2403.19887

[19] L. Ren, Y. Liu, Y. Lu, Y. Shen, C. Liang, and W. Chen, "Samba: Simple hybrid state space models for efficient unlimited context language modeling," 2025. [Online]. Available: https://arxiv.org/abs/2406.07522

[20] X. Zhu, Q. Ruan, S. Qian, and M. Zhang, "A hybrid model based on transformer and Mamba for enhanced sequence modeling," *Scientific Reports*, vol. 15, no. 1, 4 2025. [Online]. Available: https://www.nature.com/articles/s41598-025-87574-8

[21] E. Soares, N. Park, E. V. Brazil, and V. Y. Shirasuna, "A large Encoder-Decoder Polymer-Based foundation model." [Online]. Available: https://openreview.net/forum?id=bptYWF8Uy6

[22] S. Kim, J. Chen, T. Cheng, A. Gindulyte, J. He, S. He, Q. Li, B. A. Shoemaker, P. A. Thiessen, B. Yu *et al.*, "Pubchem 2023 update," *Nucleic acids research*, vol. 51, no. D1, pp. D1373–D1380, 2023.

[23] V. Sharma, M. Giammona, D. Zubarev, A. Tek, K. Nugyuen, L. Sundberg, D. Congiu, and Y.-H. La, "Formulation graphs for mapping structure-composition of battery electrolytes to device performance," *Journal of Chemical Information and Modeling*, vol. 63, no. 22, pp. 6998–7010, 2023, pMID: 37948621. [Online]. Available: https://doi.org/10.1021/acs.jcim.3c01030

[24] P. Schwaller, T. Gaudin, D. Lányi, C. Bekas, and T. Laino, ""Found in Translation": predicting outcomes of complex organic chemistry reactions using neural sequence-to-sequence models," *Chemical Science*, vol. 9, no. 28, pp. 6091–6098, 1 2018. [Online]. Available: https://pubs.rsc.org/en/content/articlelanding/2018/sc/c8sc02339e

[25] P. Schwaller, T. Laino, T. Gaudin, P. Bolgar, C. A. Hunter, C. Bekas, and A. A. Lee, "Molecular transformer: a model for uncertainty-calibrated chemical reaction prediction," *ACS central science*, vol. 5, no. 9, pp. 1572–1583, 2019.

[26] R. Irwin, S. Dimitriadis, J. He, and E. J. Bjerrum, "Chemformer: a pre-trained transformer for computational chemistry," *Machine Learning: Science and Technology*, vol. 3, no. 1, p. 015022, 2022.

[27] J. Ross, B. Belgodere, V. Chenthamarakshan, I. Padhi, Y. Mroueh, and P. Das, "Large-scale chemical language representations capture molecular structure and properties," *Nature Machine Intelligence*, vol. 4, no. 12, pp. 1256–1264, 12 2022. [Online]. Available: https://www.nature.com/articles/s42256-022-00580-7

[28] M. Aldeghi and C. W. Coley, "A graph representation of molecular ensembles for polymer property prediction," *Chemical Science*, vol. 13, no. 35, pp. 10 486–10 498, 2022.

[29] J. Yang, L. Tao, J. He, J. R. McCutcheon, and Y. Li, "Machine learning enables interpretable discovery of innovative polymers for gas separation membranes," *Science Advances*, vol. 8, no. 29, p. eabn9545, 2022.

[30] Z. Long, H. Lu, and Z. Zhang, "Large-scale glass-transition temperature prediction with an equivariant neural network for screening polymers," *ACS omega*, vol. 9, no. 5, pp. 5452–5462, 2024.

[31] M. Reis, F. Gusev, N. G. Taylor, S. H. Chung, M. D. Verber, Y. Z. Lee, O. Isayev, and F. A. Leibfarth, "Machine-learning-guided discovery of 19f mri agents enabled by automated copolymer synthesis," *Journal of the American Chemical Society*, vol. 143, no. 42, pp. 17 677–17 689, 2021.

[32] S. P. Tiwari, W. Shi, S. Budhathoki, J. Baker, A. K. Sekizkardes, L. Zhu, V. A. Kusuma, D. P. Hopkinson, and J. A. Steckel, "Creation of polymer datasets with targeted backbones for screening of high-performance membranes for gas separation," *Journal of Chemical Information and Modeling*, vol. 64, no. 3, pp. 638–652, 2024.

[33] R. Giro, H. Hsu, A. Kishimoto, T. Hama, R. F. Neumann, B. Luan, S. Takeda, L. Hamada, and M. B. Steiner, "Ai powered, automated discovery of polymer membranes for carbon capture," *npj Computational Materials*, vol. 9, no. 1, p. 133, 2023.

[34] L. Tao, V. Varshney, and Y. Li, "Benchmarking Machine Learning Models for Polymer Informatics: An Example of Glass Transition Temperature," *Journal of Chemical Information and Modeling*, vol. 61, no. 11, pp. 5395–5413, Nov. 2021. [Online]. Available: https://doi.org/10.1021/acs.jcim.1c01031

[35] S. Lo, M. Seifrid, T. Gaudin, and A. Aspuru-Guzik, "Augmenting Polymer Datasets by Iterative Rearrangement," *Journal of Chemical Information and Modeling*, vol. 63, no. 14, pp. 4266–4276, Jul. 2023, publisher: American Chemical Society. [Online]. Available: https://doi.org/10.1021/acs.jcim.3c00144

[36] K. Hatakeyama-Sato, S. Watanabe, N. Yamane, Y. Igarashi, and K. Oyaizu, "Using gpt-4 in parameter selection of polymer informatics: improving predictive accuracy amidst data scarcity and 'ugly duckling'dilemma," *Digital Discovery*, vol. 2, no. 5, pp. 1548–1557, 2023.

[37] X. Huang, S. Ma, C. Y. Zhao, H. Wang, and S. Ju, "Exploring high thermal conductivity polymers via interpretable machine learning with physical descriptors," *npj Computational Materials*, vol. 9, no. 1, pp. 1–14, Oct. 2023, publisher: Nature Publishing Group. [Online]. Available: https://www.nature.com/articles/s41524-023-01154-w

[38] G. Bradford, J. Lopez, J. Ruza, M. A. Stolberg, R. Osterude, J. A. Johnson, R. Gomez-Bombarelli, and Y. Shao-Horn, "Chemistry-informed machine learning for polymer electrolyte discovery," *ACS Central Science*, vol. 9, no. 2, pp. 206–216, 2023.

[39] C. Xu, Y. Wang, and A. Barati Farimani, "Transpolymer: a transformer-based language model for polymer property predictions," *npj Computational Materials*, vol. 9, no. 1, p. 64, 2023.

[40] M. Lewis, Y. Liu, N. Goyal, M. Ghazvininejad, A. Mohamed, O. Levy, V. Stoyanov, and L. Zettlemoyer, "BART: denoising sequence-to-sequence pre-training for natural language generation, translation, and comprehension," *CoRR*, vol. abs/1910.13461, 2019. [Online]. Available: http://arxiv.org/abs/1910.13461

[41] T. Dao and A. Gu, "Transformers are ssms: Generalized models and efficient algorithms through structured state space duality," 2024. [Online]. Available: https://arxiv.org/abs/2405.21060

[42] J. Devlin, M.-W. Chang, K. Lee, and K. Toutanova, "Bert: Pre-training of deep bidirectional transformers for language understanding," in *North American Chapter of the Association for Computational Linguistics*, 2019. [Online]. Available: https://api.semanticscholar.org/CorpusID:52967399

[43] T. Chen, T. He, M. Benesty, V. Khotilovich, Y. Tang, H. Cho, K. Chen, R. Mitchell, I. Cano, T. Zhou *et al.*, "Xgboost: extreme gradient boosting," *R package version 0.4-2*, vol. 1, no. 4, pp. 1–4, 2015.

[44] T. Akiba, S. Sano, T. Yanase, T. Ohta, and M. Koyama, "Optuna: A next-generation hyperparameter optimization framework," in *Proceedings of the 25th ACM SIGKDD international conference on knowledge discovery & data mining*, 2019, pp. 2623–2631.

[45] J. Hu, Z. Li, J. Lin, and L. Zhang, "Prediction and interpretability of glass transition temperature of homopolymers by data-augmented graph convolutional neural networks," *ACS Applied Materials & Interfaces*, vol. 15, no. 46, pp. 54 006–54 017, 2023.

[46] C. Kuenneth, A. C. Rajan, H. Tran, L. Chen, C. Kim, and R. Ramprasad, "Polymer informatics with multi-task learning," *Patterns*, vol. 2, no. 4, 2021.

[47] S. Liu, H. Wang, W. Liu, J. Lasenby, H. Guo, and J. Tang, "Pre-training molecular graph representation with 3d geometry," *arXiv preprint arXiv:2110.07728*, 2021.

[48] X. Fang, L. Liu, J. Lei, D. He, S. Zhang, J. Zhou, F. Wang, H. Wu, and H. Wang, "Geometry-enhanced molecular representation learning for property prediction," *Nature Machine Intelligence*, vol. 4, no. 2, pp. 127–134, 2022.

[49] Y. Rong, Y. Bian, T. Xu, W. Xie, Y. Wei, W. Huang, and J. Huang, "Self-supervised graph transformer on large-scale molecular data," *Advances in Neural Information Processing Systems*, vol. 33, pp. 12 559–12 571, 2020.

[50] W. Ahmad, E. Simon, S. Chithrananda, G. Grand, and B. Ramsundar, "Chemberta-2: Towards chemical foundation models," *arXiv preprint arXiv:2209.01712*, 2022.

[51] R. Taylor, M. Kardas, G. Cucurull, T. Scialom, A. Hartshorn, E. Saravia, A. Poulton, V. Kerkez, and R. Stojnic, "Galactica: A large language model for science," *arXiv preprint arXiv:2211.09085*, 2022.

[52] G. Zhou, Z. Gao, Q. Ding, H. Zheng, H. Xu, Z. Wei, L. Zhang, and G. Ke, "Uni-mol: a universal 3d molecular representation learning framework," *ChemRxiv preprint*, 2023.

[53] Y. Wang, J. Wang, Z. Cao, and A. Barati Farimani, "Molecular contrastive learning of representations via graph neural networks," *Nature Machine Intelligence*, vol. 4, no. 3, pp. 279–287, 2022.

[54] J. Chang and J. C. Ye, "Bidirectional generation of structure and properties through a single molecular foundation model," *Nature Communications*, vol. 15, no. 1, p. 2323, 2024.

[55] X. Zhang, C. Chen, X. Wang, H. Jiang, W. Zhao, and X. Cui, "MetaGIN: a lightweight framework for molecular property prediction," *Frontiers of Computer Science*, vol. 19, no. 5, 11 2024. [Online]. Available: https://doi.org/10.1007/s11704-024-3784-y

[56] K. Yang, K. Swanson, W. Jin, C. Coley, P. Eiden, H. Gao, A. Guzman-Perez, T. Hopper, B. Kelley, M. Mathea *et al.*, "Analyzing learned molecular representations for property prediction," *Journal of chemical information and modeling*, vol. 59, no. 8, pp. 3370–3388, 2019.

[57] S. Liu, M. F. Demirel, and Y. Liang, "N-gram graph: Simple unsupervised representation for graphs, with applications to molecules," *Advances in neural information processing systems*, vol. 32, 2019.

[58] W. Hu, B. Liu, J. Gomes, M. Zitnik, P. Liang, V. Pande, and J. Leskovec, "Strategies for pre-training graph neural networks," *arXiv preprint arXiv:1905.12265*, 2019.

[59] Z. Hu, Y. Dong, K. Wang, K.-W. Chang, and Y. Sun, "Gpt-gnn: Generative pre-training of graph neural networks," in *Proceedings of the 26th ACM SIGKDD international conference on knowledge discovery & data mining*, 2020, pp. 1857–1867.

[60] C. Kuenneth and R. Ramprasad, "polyBERT: a chemical language model to enable fully machine-driven ultrafast polymer informatics," *Nature Communications*, vol. 14, no. 1, p. 4099, Jul. 2023, publisher: Nature Publishing Group. [Online]. Available: https://www.nature.com/articles/s41467-023-39868-6

A   Supplementary Materials

A.1   Property prediction benchmarks details

Here, we provide detailed results for all the property prediction experiments conducted in this paper. To ensure the robustness of our claims, we conducted all experiments with five different seeds. For training models with pre-trained weights, we utilized XGBoost (43) as the learner and Optuna (44) for hyper-parameter optimization. All experiments with pre-trained models were conducted using a single NVIDIA A100 (40G) GPU.

For fine-tuning STR-Bamba$_{426M}$, we used a fully connected network with 2 layers using a single NVIDIA A100 (40G) GPU. Tables 3, and 4 provide a detailed overview of small and polymer molecules benchmark datasets used in our experiments, respectively.

Table 3: Evaluated small molecular datasets description

Dataset	Description	# compounds	# tasks	Metric
BBBP	Blood brain barrier penetration dataset	2039	1	ROC-AUC
HIV	Ability of small molecules to inhibit HIV replication	41127	1	ROC-AUC
BACE	Binding results for a set of inhibitors for β – secretase 1	1513	1	ROC-AUC
Clintox	Clinical trial toxicity of drugs	1478	2	ROC-AUC
SIDER	Drug side effect on different organ classes	1427	27	ROC-AUC
Tox21	Toxicity measurements on 12 different targets	7831	12	ROC-AUC
QM9	12 quantum mechanical calculations	133885	12	Average MAE
QM8	12 excited state properties of small molecules	21786	12	Average MAE
ESOL	Water solubility dataset	1128	1	RMSE
FreeSolv	Hydration free energy of small molecules in water	642	1	RMSE
Lipophilicity	Octanol/water distribution coefficient of molecules	4200	1	RMSE

Table 4: Evaluated polymer molecular datasets description

Dataset	Description	Metric	Source
Copolymers (MIT)	DFTB computed electron affinity and ionization potential of copolymers.	RMSE	(28)
IBM-Membrane	Computed thermal and gas permeability properties of polymers.	R^2	(33)
ACS-AMI-Homopolymer-Tg	Tg of homopolymers	RMSE	(45)
Polymer-Refractive-Index	Polymer refractive index	RMSE	(36)
Polymer-Electrolyte-Conductivity (MIT)	Conductivity of polymers and polymer formulations	MAE	(38)
Polymer-Gas-Permeability (NETL)	Gas permeability and selectivity of polymers	MAE	(32)
Polymer-Gas-Permeability (CalTech)	Gas permeability of polymers	R^2	(29)
Polyimide-Tg	Tg of polyimides	MAE	(30)
Polymer-Chain-Bandgap-(Egc)	DFT computed polymer chain bandgap	RMSE	(46; 39)
Polymer-Electron-Affinity-(Eea)	DFT computed electron affinity of polymers	RMSE	(46; 39)
Polymer-Bulk-Bandgap-(Egb)	DFT computed bulk bandgap of polymers	RMSE	(46; 39)
Polymer-Ionization-Energy-(Ei)	DFT computed ionization energy of polymers	RMSE	(46; 39)
Polymer-Dielectric-Constant-(EPS)	DFT computed dielectric constant of polymers	RMSE	(46; 39)
Polymer-Refractive-Index-(Nc)	DFT computed refractive index of polymers	RMSE	(46; 39)
Polymer-Crystallization-Tendency-(Xc)	DFT computed crystallization tendency of polymers	RMSE	(46; 39)
Polymer-Conductivity-(PE-II)	Conductivity of polymers	RMSE	(39)

A.2 Detailed results - full comparison with SOTA models in MoleculeNet benchmark

We provide the detailed comparison with the SOTA models in the MoleculeNet benchmark. Thus, Table 5 and 6 show the full comparison with the STR-Bamba$_{426M}$ pre-trained and fine-tuned models in the classification and regression tasks, respectively. These tables show the best performing results.

Table 5: Methods and Performance for the classification tasks of MoleculeNet benchmark datasets. **Blue** and **Orange** indicates best and second-best performing model, respectively.

Method	Dataset					
	BBBP	ClinTox	HIV	BACE	SIDER	Tox21
GraphMVP (47)	72.4±1.6	79.1±2.8	77.0±1.2	81.2±0.9	63.9±1.2	75.9±0.5
GEM (48)	72.4±0.4	90.1±1.3	80.6±0.9	85.6±1.1	67.2±0.4	78.1±0.1
GROVER$_{Large}$ (49)	69.5±0.1	76.2±3.7	68.2±1.1	81.0±1.4	65.4±0.1	73.5±0.1
ChemBerta (6)	64.3	90.6	62.2	-	-	-
ChemBerta2 (50)	71.94	90.7	-	85.1	-	-
Galatica 30B (51)	59.6	82.2	75.9	72.7	61.3	68.5
Galatica 120B (51)	66.1	82.6	74.5	61.7	63.2	68.9
Uni-Mol (52)	72.9±0.6	91.9±1.8	80.8±0.3	85.7±0.2	65.9±1.3	79.6±0.5
MolCLR$_{GIN}$ (53)	73.6±0.5	93.2±1.7	80.6±1.1	*89.0±0.3*	*68.0±1.1*	79.8±0.7
MolFM (52)	72.9±0.1	79.7±1.6	78.8±1.1	83.9±1.1	64.2±0.9	77.2±0.7
MoLFormer (54)	73.6±0.8	91.2±1.4	80.5±1.65	86.3±0.6	65.5±0.2	80.46±0.2
MetaGIN (55)	91.7±1.8	*90.8±8.1*	-	-	64.5±2.4	83.0±0.1
SMI-TED289M (9)	92.26±0.57	94.27±1.83	80.51±1.34	88.24±0.50	66.01±0.88	81.85±1.42
SMI-SSED$_{336M}$ (17)	92.81±0.27	90.02±0.5	83.14±0.34	86.12±0.96	63.17±0.75	*83.84±0.2*
STR-Bamba$_{426M}$ (Pre-trained)	*93.85±0.5*	93.32±0.9	*83.14±0.62*	85.6±0.67	66.42±0.38	81.57±0.37
STR-Bamba$_{426M}$ (Fine-tuned)	**94.30±0.61**	**96.44±0.07**	**84.77±0.46**	**89.84±0.23**	**69.41±0.62**	**85.02±0.65**

Table 6: Methods and Performance for the regression tasks of MoleculeNet benchmark datasets. **Blue** and **Orange** indicates best and second-best performing model, respectively.

Method	Dataset				
	QM9	QM8	ESOL	FreeSolv	Lipophilicity
D-MPNN (56)	3.241±0.119	0.0143±0.0022	0.98±0.26	2.18±0.91	0.65±0.05
N-Gram (57)	2.51±0.19	0.032±0.003	1.074±0.107	2.688±0.085	0.812±0.028
PretrainGNN (58)	-	-	1.100±0.006	2.764±0.002	0.739±0.003
GROVER$_{Large}$ (49)	-	-	0.895±0.017	2.272±0.051	0.823±0.010
ChemBERTa-2 (50)	-	-	0.89	-	0.80
SPMM (54)	-	-	0.818±0.008	1.907±0.058	0.692±0.008
MolCLR$_{GIN}$ (53)	2.357±0.118	0.0174±0.0013	1.11±0.01	2.20±0.20	0.65±0.08
Hu et al. (59)	4.349±0.061	0.0191±0.0003	1.22±0.02	2.83±0.12	0.74±0.00
MoLFormer (54)	1.5894±0.0567	*0.0102*	0.880±0.028	2.342±0.052	0.700±0.012
MetaGIN (55)	-	-	0.780±0.061	1.397±0.062	**0.532±0.013**
SMI-TED289M (9)	**1.3246±0.0157**	**0.0095±0.0001**	0.6112±0.0096	**1.2233±0.0029**	**0.5522±0.0194**
SMI-SSED$_{336M}$ (17)	2.2175±0.3194	0.0104±0.0001	0.7222±0.0139	1.6374±0.0682	0.6048±0.0023
STR-Bamba$_{426M}$ (Pre-trained)	6.8618±0.0538	0.0176±0.0002	*0.6199±0.0457*	1.3989±0.0837	0.6825±0.0061
STR-Bamba$_{426M}$ (Fine-tuned)	*1.5574±0.0156*	0.0104±0.0001	**0.5585±0.0201**	0.9426±0.0412	0.5741±0.0073

A.3 Detailed results - individual and combined molecular representations in MoleculeNet benchmark

Here we detail the results in the MoleculeNet benchmark for each molecular representation and the top-3 combination of small molecule notations. The results for each modality using pre-trained and fine-tuned models are shown in Tables 7 and 8 for classification and regression tasks, respectively.

We used TPE optimization by evaluating the validation set to find the top-3 combinations of molecular representations that demonstrate the best performance for each task. The optimization process was repeated with three different seeds for each task to ensure the statistical validity of the results. To obtain a single combination for the repeated optimization steps, we performed an intersection of the top combinations between each optimization execution. Hence, combination 1 shows the top-1 combination, combination 2 show the top-2 and combination 3 show the top-3 combination. To separate each chemical representation for the fused molecular input, we used the *<sep>* special token between them. Furthermore, in the sentence embedding from the encoder embedding layer, the first molecule notation was represented as the molecule *A* and the remaining notations as the molecule or a series of molecules *B*.

Finally, we also provide each molecular combination for the top combinations used in the evaluated tasks in the MoleculeNet benchmark. Tables 9, 10, and 11 show the combinations for top-1, top-2, and top-3, respectively. For molecular combinations, we tried all the possible combinations where the order was considered and individual representations are also included, yielding 325 possible combinations.

Table 7: Individual and combined molecular representations performance for the classification tasks of MoleculeNet benchmark datasets

Representation	Method	Dataset					
		BBBP	ClinTox	HIV	BACE	SIDER	Tox21
Molecular Formula	Pre-trained	87.67±0.39	90.22±0.50	71.86±1.01	77.49±0.16	63.61±0.73	74.67±0.86
Canonical SMILES	Pre-trained	91.27±0.37	91.0±0.71	80.98±0.69	85.60±0.67	66.42±0.38	80.33±0.39
IUPAC Name	Pre-trained	93.85±0.50	85.28±1.60	83.14±0.62	69.19±1.44	65.05±0.53	80.11±0.90
InChI	Pre-trained	91.08±0.32	85.42±1.50	78.17±0.95	84.04±0.66	63.56±0.65	79.07±0.46
SELFIES	Pre-trained	90.66±0.57	93.32±0.90	79.91±0.97	85.18±0.75	65.83±0.38	79.85±0.72
Combination 1	Pre-trained	93.85±0.50	90.69±1.0	81.30±1.37	85.35±0.58	66.42±0.38	81.57±0.37
Combination 2	Pre-trained	90.73±0.46	91.79±0.96	81.47±0.76	85.60±0.67	65.60±0.44	81.23±0.70
Combination 3	Pre-trained	91.25±1.02	91.24±0.85	82.78±0.86	83.82±1.40	65.16±0.31	81.21±0.47
Molecular Formula	Fine-tuned	87.74±0.28	87.85±0.39	72.75±0.59	75.99±1.37	63.05±1.39	80.09±0.39
Canonical SMILES	Fine-tuned	92.45±0.78	94.77±0.73	80.88±1.42	86.94±0.95	67.03±0.76	85.07±0.30
IUPAC Name	Fine-tuned	92.15±0.80	91.11±0.80	79.46±1.58	69.91±1.63	67.49±0.91	83.41±0.46
InChI	Fine-tuned	91.31±0.55	90.30±1.20	77.29±0.96	81.91±1.66	63.47±0.74	82.45±0.19
SELFIES	Fine-tuned	91.85±0.74	96.06±0.31	81.91±0.37	87.15±0.31	66.41±1.06	84.39±0.33
Combination 1	Fine-tuned	92.15±0.80	94.81±1.29	84.44±0.31	88.15±0.62	67.03±0.76	85.14±0.51
Combination 2	Fine-tuned	92.93±0.48	96.44±0.07	84.77±0.46	86.94±0.95	69.41±0.62	85.16±0.36
Combination 3	Fine-tuned	94.30±0.61	95.32±0.93	84.46±0.65	89.84±0.23	68.19±0.55	85.02±0.65

Table 8: Individual and combined molecular representations performance for the regression tasks of MoleculeNet benchmark datasets

Representation	Method	Dataset				
		QM9	QM8	ESOL	FreeSolv	Lipophilicity
Molecular Formula	Pre-trained	13.3875±0.0037	0.0297±0.0001	0.6694±0.0152	1.7005±0.0556	0.8124±0.0082
Canonical SMILES	Pre-trained	6.8618±0.0538	0.0176±0.0002	0.6439±0.0219	1.5269±0.0850	0.6888±0.0066
IUPAC Name	Pre-trained	20.7505±0.0209	0.0245±0.0001	0.8039±0.0243	1.7784±0.0472	0.7071±0.0031
InChI	Pre-trained	6.8553±0.0388	0.0210±0.0003	0.7048±0.0127	1.7284±0.0831	0.7289±0.0330
SELFIES	Pre-trained	6.6983±0.0257	0.0178±0.0004	0.6679±0.0179	1.6113±0.0916	0.7096±0.0076
Combination 1	Pre-trained	6.5891±0.0355	0.0194±0.0008	0.6199±0.0457	1.4586±0.070	0.6950±0.0087
Combination 2	Pre-trained	6.8737±0.0260	0.0220±0.0020	0.6302±0.0103	1.5482±0.0721	0.6825±0.0061
Combination 3	Pre-trained	6.8363±0.0406	0.0232±0.0024	0.6346±0.0261	1.3989±0.0837	0.6867±0.0099
Molecular Formula	Fine-tuned	12.9819±0.0092	0.0257±0.00003	0.7719±0.0348	1.7220±0.1481	0.8787±0.0239
Canonical SMILES	Fine-tuned	1.5574±0.0156	0.0107±0.0001	0.6073±0.0190	1.0909±0.0325	0.5741±0.0073
IUPAC Name	Fine-tuned	18.347±0.0110	0.0193±0.0001	0.9553±0.0207	1.6983±0.0366	0.6392±0.0096
InChI	Fine-tuned	2.3886±0.0619	0.0161±0.0001	0.7262±0.0256	1.2892±0.0216	0.6988±0.0115
SELFIES	Fine-tuned	1.5950±0.0302	0.0111±0.0001	0.6346±0.0317	1.2546±0.0678	0.6063±0.0104
Combination 1	Fine-tuned	1.5732±0.0338	0.0105±0.0001	0.5683±0.0168	0.9426±0.0412	0.5857±0.0032
Combination 2	Fine-tuned	1.7374±0.0262	0.0104±0.0001	0.5514±0.0087	1.1049±0.1087	0.5914±0.0021
Combination 3	Fine-tuned	1.6183±0.0267	0.0104±0.0001	0.5585±0.0201	1.1105±0.0587	0.5814±0.0073

A.4 Detailed results - polymer property prediction tasks

Here we provide the detailed results of the nine polymer prediction tasks in which the R^2 metric was used and the results for the remaining 17 polymer property prediction tasks, resulting in a total of 26 polymer downstream tasks.

Table 9: Top-1 molecular combinations for the MoleculeNet benchmark datasets.

Dataset	Task	Molecular combination
BBBP	p_np	IUPAC_NAME
ClinTox	all	INCHI + MOLECULAR_FORMULA + IUPAC_NAME + SELFIES + CANONICAL_SMILES
HIV	HIV_active	CANONICAL_SMILES + SELFIES + MOLECULAR_FORMULA + INCHI + IUPAC_NAME
BACE	Class	IUPAC_NAME + MOLECULAR_FORMULA + SELFIES + INCHI + CANONICAL_SMILES
SIDER	all	CANONICAL_SMILES
Tox21	all	IUPAC_NAME + MOLECULAR_FORMULA + INCHI + CANONICAL_SMILES + SELFIES
QM9	alpha	IUPAC_NAME + SELFIES + MOLECULAR_FORMULA + INCHI
QM9	cv	SELFIES + MOLECULAR_FORMULA + INCHI
QM9	g298	SELFIES + MOLECULAR_FORMULA + INCHI + CANONICAL_SMILES
QM9	gap	CANONICAL_SMILES
QM9	h298	SELFIES + MOLECULAR_FORMULA + INCHI + IUPAC_NAME + CANONICAL_SMILES
QM9	homo	CANONICAL_SMILES
QM9	lumo	CANONICAL_SMILES
QM9	mu	CANONICAL_SMILES
QM9	r2	MOLECULAR_FORMULA + INCHI + SELFIES + CANONICAL_SMILES
QM9	u0	SELFIES + MOLECULAR_FORMULA + INCHI + IUPAC_NAME + CANONICAL_SMILES
QM9	u298	SELFIES + MOLECULAR_FORMULA + INCHI + IUPAC_NAME + CANONICAL_SMILES
QM9	zpve	SELFIES + MOLECULAR_FORMULA + INCHI + CANONICAL_SMILES
QM8	E1-CAM	CANONICAL_SMILES
QM8	E1-CC2	SELFIES + MOLECULAR_FORMULA + INCHI + CANONICAL_SMILES
QM8	E1-PBE0	CANONICAL_SMILES
QM8	E2-CAM	CANONICAL_SMILES
QM8	E2-CC2	CANONICAL_SMILES
QM8	E2-PBE0	CANONICAL_SMILES
QM8	f1-CAM	CANONICAL_SMILES
QM8	f1-CC2	SELFIES + CANONICAL_SMILES
QM8	f1-PBE0	MOLECULAR_FORMULA + CANONICAL_SMILES + IUPAC_NAME
QM8	f2-CAM	CANONICAL_SMILES
QM8	f2-CC2	CANONICAL_SMILES + IUPAC_NAME + MOLECULAR_FORMULA + SELFIES
QM8	f2-PBE0	CANONICAL_SMILES
ESOL	log solubility	IUPAC_NAME + MOLECULAR_FORMULA + SELFIES + INCHI + CANONICAL_SMILES
FreeSolv	expt	SELFIES + CANONICAL_SMILES + MOLECULAR_FORMULA + INCHI
Lipophilicity	y	SELFIES + MOLECULAR_FORMULA + INCHI + IUPAC_NAME + CANONICAL_SMILES

Table 10: Top-2 molecular combinations for the MoleculeNet benchmark datasets.

Dataset	Task	Molecular combination
BBBP	p_np	SELFIES + CANONICAL_SMILES
ClinTox	all	CANONICAL_SMILES + IUPAC_NAME + SELFIES + MOLECULAR_FORMULA
HIV	HIV_active	IUPAC_NAME + MOLECULAR_FORMULA + INCHI + CANONICAL_SMILES
BACE	Class	CANONICAL_SMILES
SIDER	all	IUPAC_NAME + MOLECULAR_FORMULA + INCHI + CANONICAL_SMILES + SELFIES
Tox21	all	INCHI + CANONICAL_SMILES + SELFIES + IUPAC_NAME + MOLECULAR_FORMULA
QM9	alpha	MOLECULAR_FORMULA
QM9	cv	IUPAC_NAME + MOLECULAR_FORMULA + INCHI + CANONICAL_SMILES + SELFIES
QM9	g298	SELFIES + MOLECULAR_FORMULA + INCHI + IUPAC_NAME + CANONICAL_SMILES
QM9	gap	CANONICAL_SMILES + IUPAC_NAME + MOLECULAR_FORMULA + SELFIES
QM9	h298	CANONICAL_SMILES + MOLECULAR_FORMULA + IUPAC_NAME + INCHI
QM9	homo	SELFIES + CANONICAL_SMILES + INCHI + MOLECULAR_FORMULA
QM9	lumo	INCHI + CANONICAL_SMILES + SELFIES + IUPAC_NAME + MOLECULAR_FORMULA
QM9	mu	IUPAC_NAME + SELFIES + CANONICAL_SMILES + MOLECULAR_FORMULA
QM9	r2	SELFIES + INCHI + CANONICAL_SMILES + MOLECULAR_FORMULA + IUPAC_NAME
QM9	u0	CANONICAL_SMILES + MOLECULAR_FORMULA + IUPAC_NAME + INCHI
QM9	u298	CANONICAL_SMILES + MOLECULAR_FORMULA + IUPAC_NAME + INCHI
QM9	zpve	CANONICAL_SMILES + MOLECULAR_FORMULA + IUPAC_NAME + INCHI
QM8	E1-CAM	CANONICAL_SMILES + IUPAC_NAME + MOLECULAR_FORMULA + SELFIES
QM8	E1-CC2	INCHI + MOLECULAR_FORMULA + IUPAC_NAME + SELFIES + CANONICAL_SMILES
QM8	E1-PBE0	MOLECULAR_FORMULA + SELFIES + IUPAC_NAME + CANONICAL_SMILES
QM8	E2-CAM	MOLECULAR_FORMULA + SELFIES + IUPAC_NAME + CANONICAL_SMILES
QM8	E2-CC2	MOLECULAR_FORMULA + SELFIES + IUPAC_NAME + CANONICAL_SMILES
QM8	E2-PBE0	MOLECULAR_FORMULA + SELFIES + IUPAC_NAME + CANONICAL_SMILES
QM8	f1-CAM	IUPAC_NAME + CANONICAL_SMILES
QM8	f1-CC2	CANONICAL_SMILES
QM8	f1-PBE0	SELFIES + CANONICAL_SMILES + MOLECULAR_FORMULA + IUPAC_NAME
QM8	f2-CAM	CANONICAL_SMILES + IUPAC_NAME + MOLECULAR_FORMULA + SELFIES
QM8	f2-CC2	CANONICAL_SMILES
QM8	f2-PBE0	CANONICAL_SMILES + IUPAC_NAME + SELFIES + MOLECULAR_FORMULA
ESOL	log solubility	INCHI + MOLECULAR_FORMULA + SELFIES + CANONICAL_SMILES + IUPAC_NAME
FreeSolv	expt	SELFIES + MOLECULAR_FORMULA + INCHI + IUPAC_NAME + CANONICAL_SMILES
Lipophilicity	y	MOLECULAR_FORMULA + IUPAC_NAME + INCHI + CANONICAL_SMILES + SELFIES

Specifically, Tables 12 and 13 show the results for the polymer membranes and the gas permeability of polymers (CalTech) datasets, respectively. The polymer membrane prediction dataset contains three different tasks. Similarly, the gas permeability of polymers (CalTech) dataset contains six different tasks.

Table 11: Top-3 molecular combinations for the MoleculeNet benchmark datasets.

Dataset	Task	Molecular combination
BBBP	p_np	MOLECULAR_FORMULA + IUPAC_NAME + CANONICAL_SMILES + INCHI + SELFIES
ClinTox	all	IUPAC_NAME + SELFIES + MOLECULAR_FORMULA
HIV	HIV_active	MOLECULAR_FORMULA + IUPAC_NAME + CANONICAL_SMILES + INCHI + SELFIES
BACE	Class	INCHI + MOLECULAR_FORMULA + IUPAC_NAME + SELFIES + CANONICAL_SMILES
SIDER	all	SELFIES + MOLECULAR_FORMULA + IUPAC_NAME + CANONICAL_SMILES
Tox21	all	IUPAC_NAME + MOLECULAR_FORMULA + INCHI + CANONICAL_SMILES
QM9	alpha	SELFIES + MOLECULAR_FORMULA + INCHI + IUPAC_NAME + CANONICAL_SMILES
QM9	cv	CANONICAL_SMILES + MOLECULAR_FORMULA + INCHI + IUPAC_NAME + SELFIES
QM9	g298	CANONICAL_SMILES + MOLECULAR_FORMULA + IUPAC_NAME + INCHI
QM9	gap	INCHI + MOLECULAR_FORMULA + IUPAC_NAME + SELFIES + CANONICAL_SMILES
QM9	h298	INCHI + MOLECULAR_FORMULA + IUPAC_NAME + CANONICAL_SMILES + SELFIES
QM9	homo	CANONICAL_SMILES + MOLECULAR_FORMULA + IUPAC_NAME + INCHI + SELFIES
QM9	lumo	INCHI + MOLECULAR_FORMULA + IUPAC_NAME + SELFIES + CANONICAL_SMILES
QM9	mu	SELFIES + MOLECULAR_FORMULA + INCHI + IUPAC_NAME + CANONICAL_SMILES
QM9	r2	INCHI + MOLECULAR_FORMULA + IUPAC_NAME + SELFIES + CANONICAL_SMILES
QM9	u0	INCHI + MOLECULAR_FORMULA + IUPAC_NAME + CANONICAL_SMILES + SELFIES
QM9	u298	INCHI + MOLECULAR_FORMULA + IUPAC_NAME + CANONICAL_SMILES + SELFIES
QM9	zpve	IUPAC_NAME + MOLECULAR_FORMULA + INCHI + CANONICAL_SMILES + SELFIES
QM8	E1-CAM	SELFIES + MOLECULAR_FORMULA + INCHI + CANONICAL_SMILES
QM8	E1-CC2	INCHI + CANONICAL_SMILES + SELFIES + IUPAC_NAME + MOLECULAR_FORMULA
QM8	E1-PBE0	CANONICAL_SMILES + IUPAC_NAME + MOLECULAR_FORMULA + SELFIES
QM8	E2-CAM	MOLECULAR_FORMULA + IUPAC_NAME + CANONICAL_SMILES
QM8	E2-CC2	MOLECULAR_FORMULA + IUPAC_NAME + CANONICAL_SMILES
QM8	E2-PBE0	INCHI + MOLECULAR_FORMULA + IUPAC_NAME + SELFIES + CANONICAL_SMILES
QM8	f1-CAM	CANONICAL_SMILES + INCHI + SELFIES + IUPAC_NAME + MOLECULAR_FORMULA
QM8	f1-CC2	CANONICAL_SMILES + IUPAC_NAME + MOLECULAR_FORMULA + SELFIES
QM8	f1-PBE0	INCHI + MOLECULAR_FORMULA + IUPAC_NAME + SELFIES + CANONICAL_SMILES
QM8	f2-CAM	MOLECULAR_FORMULA + SELFIES + IUPAC_NAME + CANONICAL_SMILES
QM8	f2-CC2	MOLECULAR_FORMULA + IUPAC_NAME + CANONICAL_SMILES
QM8	f2-PBE0	SELFIES + CANONICAL_SMILES + MOLECULAR_FORMULA + IUPAC_NAME
ESOL	log solubility	SELFIES + MOLECULAR_FORMULA + INCHI + IUPAC_NAME + CANONICAL_SMILES
FreeSolv	expt	MOLECULAR_FORMULA + IUPAC_NAME + CANONICAL_SMILES + INCHI + SELFIES
Lipophilicity	y	IUPAC_NAME + SELFIES + CANONICAL_SMILES + INCHI + MOLECULAR_FORMULA

Table 12: Polymer membranes prediction performance. R^2 is used as evaluation metric, therefore, in this case higher values is better. **Blue** and **Orange** indicates best and second-best performing model, respectively.

Method	Dataset		
	$T_{d\frac{1}{2}}$	T_g	$\log(P_{CO_2})$
Lasso (33)	0.81	**0.90**	0.87
ElasticNet (33)	0.81	0.88	0.89
Ridge (33)	0.82	**0.90**	0.90
SPG-TED$_{289M}$ (21)	0.96	0.86	0.88
STR-Bamba$_{426M}$ (Pre-trained)	**0.98$\pm$0.001**	0.86$\pm$0.007	**0.91$\pm$0.005**
STR-Bamba$_{426M}$ (Fine-tuned)	**0.98$\pm$0.003**	**0.91$\pm$0.008**	**0.96$\pm$0.001**

Table 13: Gas permeability of polymers (CalTech) prediction. R^2 is used as evaluation metric, therefore, in this case higher values is better. **Blue** and **Orange** indicates best and second-best performing model, respectively.

Method	Dataset					
	He	H_2	O_2	N_2	CO_2	CH_4
RF (descriptors) (29)	0.73	0.74	0.75	0.74	0.38	0.75
DNN ensemble(descriptors) (29)	0.87	0.88	0.89	0.90	0.90	**0.89**
DNN ensemble(MFFs) (29)	0.91	**0.90**	**0.92**	**0.91**	0.90	0.88
SPG-TED$_{289M}$ (21)	**0.92**	0.87	0.89	**0.91**	**0.91**	0.85
STR-Bamba$_{426M}$ (Pre-trained)	0.7$\pm$0.02	0.73$\pm$0.03	0.75$\pm$0.05	0.76$\pm$0.02	0.78$\pm$0.03	0.78$\pm$0.02
STR-Bamba$_{426M}$ (Fine-tuned)	**0.92$\pm$0.01**	**0.91$\pm$0.01**	**0.91$\pm$0.004**	**0.91$\pm$0.004**	**0.90$\pm$0.01**	**0.90$\pm$0.01**

The latter of 17 polymer property prediction tasks comprises a total of six different datasets. Hence, Tables 14, 15, 16, 17, 18, and 19 show the comparison between STR-Bamba$_{426M}$ model with SOTA models for polymer ionic conductivity, gas permeability (NETL), polymer refractive index, polymer multitask prediction, copolymer electron affinity and ionization potential, and glass-transition temperature datasets, respectively.

Table 14: Polymer ionic conductivity. MAE is used as evaluation metric, therefore, in this case lower is better. **Blue** and **Orange** indicates best and second-best performing model, respectively.

Method	Dataset Polymer ionic conductivity
XGBoost (36)	1.09
Chemprop (36)	1.08
ChemArr (36)	1.00
SPG-TED$_{289M}$ (21)	0.89
STR-Bamba$_{426M}$ (Pre-trained)	0.92±0.001
STR-Bamba$_{426M}$ (Fine-tuned)	0.89±0.004

Table 15: Gas permeability of polymers (NETL) prediction. MAE is used as evaluation metric, therefore, in this case lower is better. **Blue** and **Orange** indicates best and second-best performing model, respectively.

Method	Dataset				
	CO_2	CO_2/CH_4	CH_4	CO_2/N_2	N_2
SOTA (32)	0.29	5.34	0.37	4.14	0.38
SPG-TED$_{289M}$ (21)	0.29	4.71	0.35	3.89	0.31
STR-Bamba$_{426M}$ (Pre-trained)	0.25±0.01	6.22±0.13	0.34±0.01	4.05±0.09	0.28±0.01
STR-Bamba$_{426M}$ (Fine-tuned)	0.24±0.01	4.69±0.16	0.28±0.002	3.83±0.08	0.25±0.01

Table 16: Polymer refractive index prediction. RMSE is used as evaluation metric, therefore, in this case lower is better. **Blue** and **Orange** indicates best and second-best performing model, respectively.

Method	Dataset Refractive index (n)
GPT-4 (36)	0.0310
Boruta (36)	0.0339
SPG-TED$_{289M}$ (21)	0.0210
STR-Bamba$_{426M}$ (Pre-trained)	0.0276±0.003
STR-Bamba$_{426M}$ (Fine-tuned)	0.0234±0.0057

Table 17: Polymer multi-task prediction. RMSE is used as evaluation metric, therefore, in this case lower is better. **Blue** and **Orange** indicates best and second-best performing model, respectively.

Method	Dataset						
	Polymer Chain Bandgap (Egc)	Polymer Electron Affinity (Eea)	Polymer Bulk Bandgap (Egb)	Polymer Ionization Energy (Ei)	Polymer Dielectric Constant (EPS)	Polymer Refractive Index (Nc)	Polymer Crystallization Tendency (Xc)
SOTA (60; 39)	0.44	0.28	0.49	0.39	0.52	0.09	16.57
SPG-TED$_{289M}$ (21)	0.49	0.29	0.32	0.37	0.38	0.12	17.82
STR-Bamba$_{426M}$ (Pre-trained)	0.55±0.01	0.36±0.01	0.63±0.02	0.63±0.02	0.77±0.03	0.15±0.01	22.26±1.02
STR-Bamba$_{426M}$ (Fine-tuned)	0.43±0.01	0.18±0.01	0.40±0.02	0.44±0.02	0.48±0.02	0.13±0.01	18.98±0.74

Table 18: Copolymer electron affinity and ionization potential. RMSE is used as evaluation metric, therefore, in this case lower is better. **Blue** and **Orange** indicates best and second-best performing model, respectively.

Method	Dataset	
	EA (eV)	IP (eV)
Neural Networks (Monomer) (28)	0.22	0.19
Neural Networks (Polymer) (28)	0.18	0.16
wD-MPNN (28)	0.03	0.03
SPG-TED$_{289M}$ (21)	0.15	0.16
STR-Bamba$_{426M}$ (Pre-trained)	0.21±0.001	0.20±0.001
STR-Bamba$_{426M}$ (Fine-tuned)	0.18±0.001	0.17±0.001

Table 19: Glass-transition temperature prediction. MAE is used as evaluation metric, therefore, in this case lower is better. **Blue** and **Orange** indicates best and second-best performing model, respectively.

Method	Dataset T_g (K)
SOTA (30)	53.02 (24.42)
SPG-TED$_{289M}$ (21)	9.56
STR-Bamba$_{426M}$ (Pre-trained)	4.85±0.04
STR-Bamba$_{426M}$ (Fine-tuned)	3.36±0.52